

Photothermal gas sensing with a custom-made, fiber-coupled Fabry–Pérot etalon

Manuel Tanzer^{Ⓢ,a,*} Benjamin Lang,^a Matej Njegovec,^b Vedran Budinski,^b Simon Pevec,^b Jure Javornik,^b Denis Donlagic,^b and Alexander Bergmann^a

^aGraz University of Technology, Institute for Electrical Measurement and Sensor Systems, Graz, Austria

^bUniversity of Maribor, Faculty of Electrical Engineering and Computer Science, Maribor, Slovenia

ABSTRACT. Growing awareness of the adverse health effects of air pollution has increased the demand for reliable, sensitive, and mass-producible sensor systems. Photothermal interferometry has shown great promise for sensitive, selective, and miniaturized gas sensing solutions. This work describes the development of a macroscopic photothermal sensor system with a sensor head consisting of a low-cost, custom-made, and fiber-coupled Fabry–Pérot etalon. The sensor was tested with NO₂, achieving a 3 σ limit of detection (LOD) of approximately 370 ppbv (1 s). Exhibiting little drift, a LOD of 15 ppbv is achievable for 200 s integration time. Compensating for the excitation power, the normalized noise equivalent absorption was calculated to be $1.4 \times 10^{-8} \text{ cm}^{-1} \text{ W}\sqrt{\text{Hz}}$. The sensor system is not limited to NO₂ but can be used for any gas or aerosol species by exchanging the excitation laser source.

© The Authors. Published by SPIE under a Creative Commons Attribution 4.0 International License. Distribution or reproduction of this work in whole or in part requires full attribution of the original publication, including its DOI. [DOI: [10.1117/1.OE.63.6.064101](https://doi.org/10.1117/1.OE.63.6.064101)]

Keywords: photothermal interferometry; spectroscopy; Fabry–Pérot etalon; gas sensing; nitrogen dioxide

Paper 20231238G received Dec. 23, 2023; revised Apr. 9, 2024; accepted May 20, 2024; published Jun. 4, 2024.

1 Introduction

The detection of trace concentrations of gases is crucial in countless fields of application. From environmental monitoring to leakage detection in industrial applications or in the medical sector, sensitive and selective determination of gas concentrations has to be ensured in a cost-effective way. There are many known gas sensing methods, but they either lack the necessary accuracy or do not meet the price requirements for the respective application.¹ Laser-based spectroscopic sensor systems offer the advantage of a high sensitivity and selectivity.² In tunable diode laser based absorption spectroscopy, the signal scales with the gas-laser beam interaction length according to the Beer–Lambert law. It states that the incident laser power is attenuated exponentially over the detection path length, thereby posing a limit to the miniaturization potential.³ In photothermal spectroscopy on the other hand, the signal detection can be done with interferometric precision and sensitivity, enabling the realization of just minute detection volumes.^{4–8} However, most of the photothermal interferometry (PTI) setups presented to date, are large and rather complex bench-top systems relying on the use of expensive equipment. For field application, the sensing system needs to be down-scaled and a rugged interferometric sensing unit is essential. For the characterization of the setup proposed in this work, we have chosen nitrogen dioxide (NO₂) as analyte, whose detrimental effect on both health and climate has been proven in many studies.⁹ Evidence suggests that elevated exposure levels can be associated with respiratory diseases as well as premature deaths.¹⁰ Precise monitoring of gas concentration levels is essential

*Address all correspondence to Manuel Tanzer, manuel.tanzer@tugraz.at

for raising public and political awareness to the problem of air pollution, and thus the enforcement of strict regulation standards. Optical sensors, such as photothermal and photoacoustic gas sensors, allow selective measurements and sensitivities down to the parts per billion by volume (ppbv) region have already been demonstrated.^{11–15} This work presents the characterization of a novel optical fiber-based PTI gas sensing system. Instead of relying on a commercially available and expensive Fabry–Pérot etalon (FPE), we make use of a low-cost and custom-made FPE. The etalon has been manufactured with an easily accessible fabrication method using only basic photonic equipment, available in any photonic laboratory.¹⁶ The price of commercially available high-finesse FPEs surmounts the commonly acceptable budget for prototyping. By relying on off-the-shelf bulk-optic and telecom fiber-optic components, the material costs of the FPE, as used here, could be reduced to less than 400 euros. A comparison to similar configurations is difficult, given the lack of disclosed details about the fabrication methods as well as the equipment necessary for glass processing and coating. See, e.g., reference Chen et al.¹⁷ Convenient handling of the main sensing unit is ensured by fiber-coupling the air-spaced etalon. The presented gas sensing system is calibrated with well-defined concentrations of NO₂, demonstrating its potential for various gas sensing applications. The calibration results also more generally display the favorable capabilities of the developed low-cost FPEs as a required next step toward low-cost sensitive photothermal trace gas monitoring.

2 Methods

2.1 PTI Working Principle

In PTI, minute changes in refractive index (RI), induced by exciting and thereby heating the target gas periodically via laser irradiation, are measured interferometrically.¹⁸ Careful selection of the excitation wavelength with respect to cross-sensitivities to other gases ensures a high selectivity toward the target gas while being unaffected by other gases, which may be present during the measurement. Periodic modulation of the excitation laser, either in wavelength or in intensity, leads to modulated absorption and RI changes, proportional to the gas concentration present. Neglecting excitational relaxation losses, the oscillatory temperature ΔT_{osc} and phase $\Delta\phi_{\text{osc}}$ amplitudes, induced in the gas by intensity-modulated and collimated laser irradiation, can be calculated with the following equations:¹⁸

$$\Delta T_{\text{osc}} = \frac{2\alpha P_{\text{eff}}}{\pi w^2 \rho_0 c_p \omega}, \quad \Delta n_{\text{osc}} = \frac{n_0 - 1}{T_0} \Delta T_{\text{osc}}, \quad (1)$$

where α is the absorption coefficient of the gas, P_{eff} the effective optical power of the excitation laser (peak-to-peak power), w the excitation laser's beam radius, ρ_0 and c_p the density and specific heat capacity of air, and ω is the angular excitation frequency. These changes in RI are then detected, e.g., using an FPE, as illustrated in Fig. 1. In order to perform wavelength modulation spectroscopy (WMS), distinct absorption peaks are beneficial.¹⁹ In the region around 450 nm, NO₂ exhibits strong but broad absorption features²⁰ not suitable for WMS, which is why intensity modulation was performed for the measurements presented here.

The transmittance T and reflectance $R = 1 - T$ through the FPE can be described by the Airy distribution.²¹ Depending on the reflectivity $R_m \in [0, 1]$ of the identical mirrors and the phase ϕ , the transmittance for the case of normal incidence can be written as

$$T = \frac{(1 - R_m)^2}{1 - 2R_m \cos(\phi) + R_m^2}, \quad \phi = \frac{4\pi nd}{\lambda}, \quad (2)$$

where n is the RI, d is the distance between the two mirrors, and λ is the wavelength of the etalon's probe laser. The red dotted line in Fig. 1 depicts the gradient of the function, here referred to as sensitivity $S = (\partial R / \partial \phi)$, which acts as conversion factor between the generated phase change and the subsequent change in reflected intensity. For photothermal measurements, the operation point of the interferometric detection unit is chosen to be at the inflection point of the function, where the sensitivity to phase changes is the highest. The sensitivity is proportional to the finesse of the FPE, which is commonly used as a figure of merit of an FPE. The use of such multi-pass interferometers allows miniaturization of the detection unit of a PTI sensor, by reducing the necessary gas-laser interaction path. By proper selection of the wavelength of

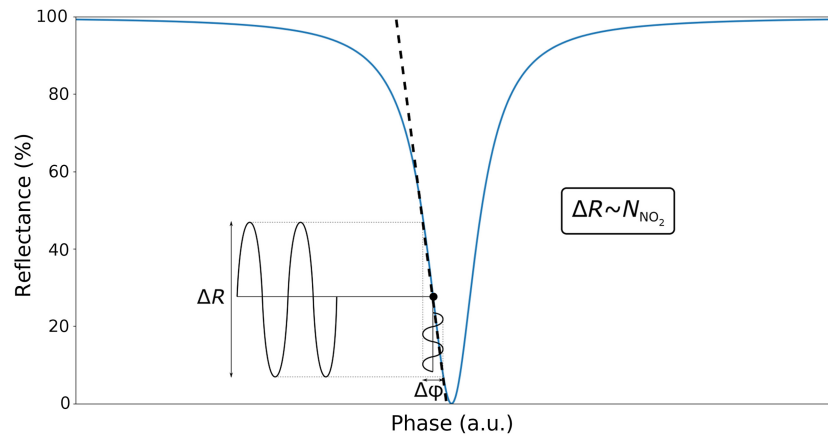


Fig. 1 Exemplary reflection function of an FPE, plotted over the phase $\phi = (4\pi nd/\lambda)$. The periodic change of RI leads to a periodic change of the phase inside the etalon and therefore a modulation of the backreflected light ΔR . Given that the slope of the function can be assumed linear (dotted line) around the inflection point (black dot), ΔR is proportional to the gas concentration N_{NO_2} .

the excitation laser, minimum cross-interferences with other gases, in terms of absorption as well as excitational relaxation pathways can be ensured. This makes PTI gas sensors highly selective and the interchangeable nature of the excitation laser allows detection of many gas and aerosol species, given the right laser source is available.

2.2 Experimental Methods

A schematic of the macroscopic sensor system is shown in Fig. 2. The fiber-optic interferometric sensing part is depicted in the lower left corner of the figure. To minimize the influence of laser phase noise on the setup, an ultra-narrow linewidth fiber-coupled laser source (NKT, E15, 1550 nm) is used as probe laser. An optical isolator (AFW Technologies, SM dual-stage isolator) is installed, to prevent back-reflections into the laser. As a balanced detection (BD) scheme is used, the light intensity is subsequently split by a 90:10 fiber-optic splitter (Agiltron, SM micro-optic coupler) into a reference and signal path. Roughly 10 % of the light is directed onto the

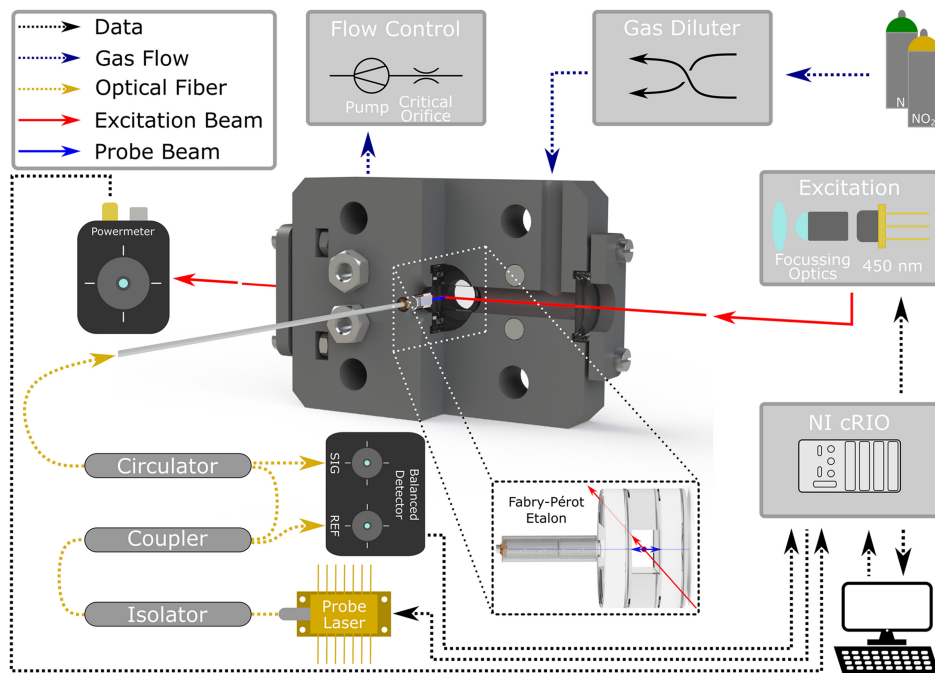


Fig. 2 A schematic of the developed macroscopic sensor system visualizing its working principle. In the center, the 3D-printed measurement cell with the integrated fiber-coupled FPE is depicted.

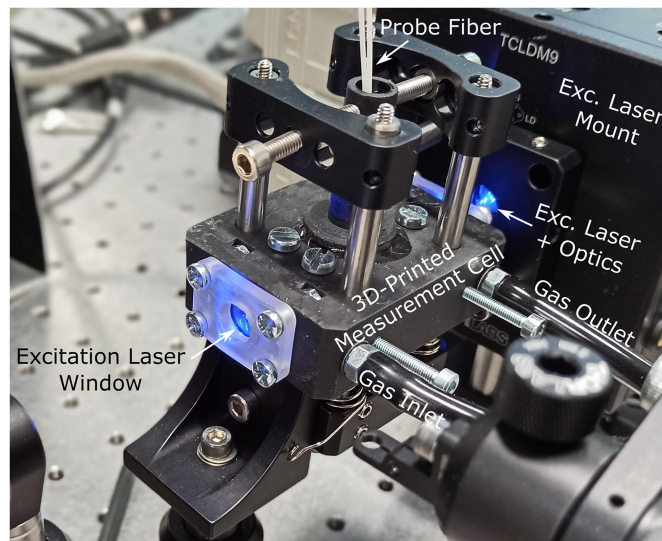


Fig. 3 Picture of the measurement cell with the excitation laser turned on.

reference photodiode of the balanced detector (Newport, Nirvana 2017), whereas the rest passes a circulator (AFW Technologies, SM circulator) before entering the FPE.

Etalons act as converter from frequency modulation, due to the laser's phase noise, to amplitude modulation (FM to AM noise). As the FPE used for detection of the photothermal signal, is only present in the signal path, BD cannot compensate for the additional amplitude noise, highlighting the need for an ultra-low-noise laser source. Alternatively, a feedback-based stabilization scheme could be implemented, e.g., Pound–Drever–Hall method, with the advantage of having a larger tolerance toward low-cost laser sources.²² However, additional optical and electrical components would be required, adding to the complexity and size of the setup. To allow interaction between the target gas and the laser light, an air-spaced FPE has to be used. As commercially available FPEs are typically expensive, a novel low-cost method to fabricate fiber-coupled, air-spaced FPEs was developed, to allow fast and easy prototyping. Details of the fabrication process can be found in Tanzer et al.¹⁶ The FPE used for the NO₂ measurements, as presented here, has a finesse of roughly 30 and a sensitivity to RI changes of $8.2 \cdot 10^6 \frac{\%}{\text{RIU}}$. Direct mounting of the FPE to a single-mode fiber collimator (DK photonics, SM fiber collimator) creates a high mechanical stability of the detection unit, without the need for re-alignment after handling of the measurement cell. A picture of the measurement cell is shown in Fig. 3.

A gradient index lens collimates the laser beam out of the fiber and collects the reflected light from the FPE. The circulator then directs the reflected light onto the signal photodiode of the balanced detector. The excitation laser (Laser Components, PLT5 450B, 450 nm, 80 mW) beam is focused perpendicularly onto the probe laser beam inside the air-spaced etalon. Two wedged windows ensure that the measurement cell is air-tight while allowing the excitation beam to pass. For data acquisition and management of the system, an FPGA-based system (NI, cRIO9031) with a 24 bit ADC (NI, 9234) is used. This system controls the laser drivers, acquires data from the detectors and also features a lock-in amplifier (LIA), which allows for phase sensitive background correction of the photothermal signal amplitude. Operation of the system is done via a custom LabView-based user interface. To maintain the probe laser's wavelength at the FPE transfer function's inflection point and ensure optimum sensitivity of the system during measurements, a PID-controller was implemented. A fast response of the controller has to be ensured, to avoid drift of the operation point when the gas concentration or composition changes throughout the measurement campaign. For the characterization of the instrument with well-defined NO₂ concentrations, a custom-made gas diluter, based on critical orifices, is used, to dilute 1000 ppmv of NO₂ with pure nitrogen N₂ down to the desired concentration levels.²³ As abrupt changes of the flow rate can lead to a strong drift of the operation point, a pump in combination with a critical orifice (0.249 slm) is installed downstream of the cell. Together with a venting tube upstream of the cell, constant flow through the FPE is ensured. For environmental

sensing applications however, fast changes of pressure and flow rate through the system can be avoided, making the use of these additional components obsolete. To achieve maximum sensitivity, the operation parameters of the setup were determined in the following way: with the maximum NO_2 concentration present in the measurement cell, a frequency sweep of the intensity modulated excitation laser (50% duty cycle) was performed, to determine the optimal excitation frequency. As longer integration times lower the limit of detection (LOD), stability measurements were performed for more than 1 h. By calculating the Allan deviation, the maximum integration time was determined.^{24,25}

3 Results

By comparing the measured signal-to-noise ratios (SNRs) obtained via the frequency sweep, the ideal excitation frequency f_{exc} was determined, as depicted in Fig. 4. The fluctuations in the measured data points can be attributed to the limited integration time of the LIA of 5 s. Repeated measurements for the regions of interest around 650 and 1100 nm with an integration time of 10 s revealed an optimum excitation frequency of 1065 Hz.

In Fig. 5, the measured background-corrected lock-in amplitude for an integration time τ_{int} of 1 s is shown over the NO_2 concentration as set by the gas diluter.

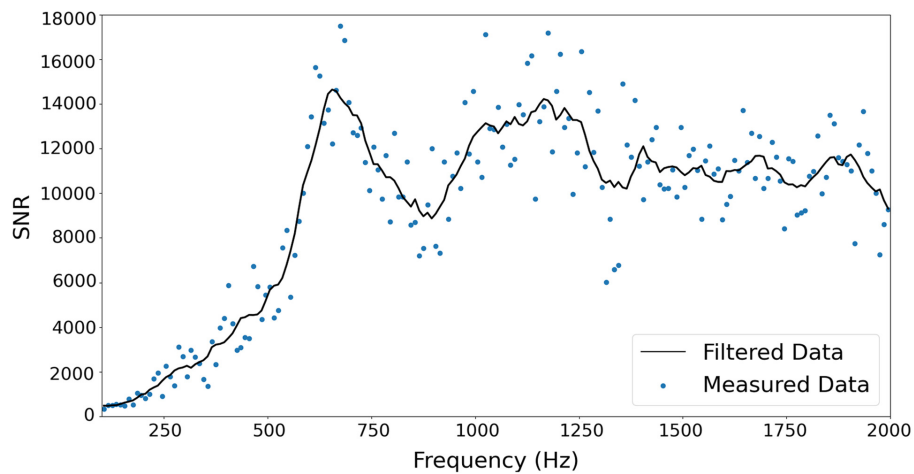


Fig. 4 The SNRs as obtained by sweeping the excitation frequency from 100 to 2000 Hz during measurements of 1000 ppmv of NO_2 with 5 s integration time.

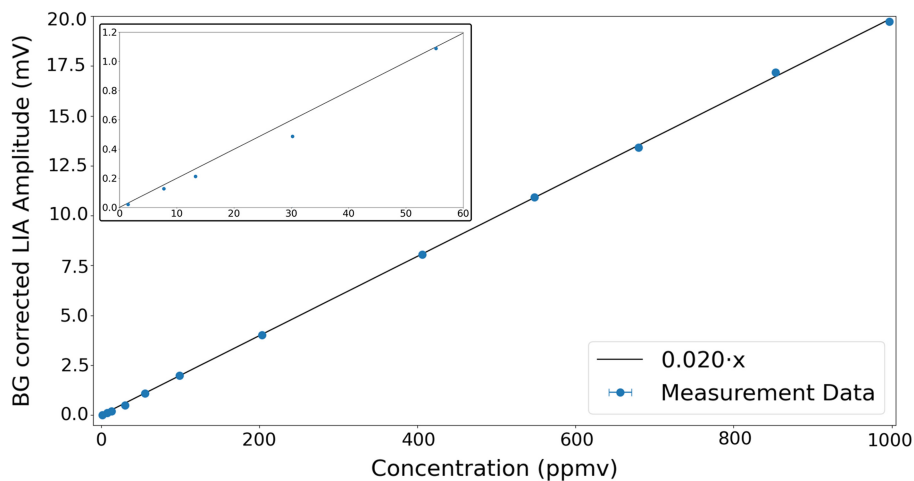


Fig. 5 The measured LIA amplitude for different NO_2 concentrations with 1 s integration time. The black line is a linear fit and indicates the linearity of the sensor system. As only one measurement was performed per data point, no standard deviation can be given. The uncertainties of the gas concentrations are too small to be visible in the plot.

Table 1 Main sources of uncertainty of the measurement results.

	Sources of uncertainty	Brief description	Weight
Gas	Gas bottle concentration	997 ppmv of NO ₂ with 2 % uncertainty	****
	Gas diluter	Uncertainty of mixing ratio (0.1% to 1.2%)	****
	Incomplete gas exchange	Long required flushing times of tubing and dead volumes, especially for low concentrations	****
System	Sensitivity fluctuations	Variable conditions (p, T, n) can change the slope of the FPE	**
	Exc. laser power instability	Fluctuating optical power emitted by exc. laser	**
	Mechanical instabilities	Variable optical alignment can change overlap between exc. and probe laser	*
	Fiber-optical components	Unwanted interference effects changing the reflected optical power	*
	Probe laser noise	Phase noise, relative intensity noise, etc.	*
	Electronics noise	Laser drivers, detectors, data acquisition, etc.	*

The black line is a first order polynomial fit with zero offset, indicating the linearity of the sensor system. The inset on the upper left side of the plot shows the low concentration region up to 60 ppmv. As only one measurement per data point was performed, no statistical evaluation can be given.

The main source of uncertainty in the measurement results can be attributed to the reference system, namely the gas diluter and the subsequent tubing system for supplying gas to the measurement cell. The uncertainties of the concentrations, as given by the gas diluter, are plotted as errorbars in x-direction, however, they are too small to be visible in the graph. The deviations from the linear fit, especially in the low concentration regions, are mainly stemming from insufficient gas exchange times. The long tubing and possible dead volumes in the measurement cell demand flushing times for multiple hours, which was not practical during the measurement campaign. As no reference sensor was used, no quantification thereof can be given at this point. In Table 1 a list of sources adding to the uncertainty of the measurement is given, together with a ranking in terms of relative weight of the respective source. For most of the indicated sources, mitigation measures have been taken. To address fluctuations of the sensitivity of the FPE, a PID-controller based operation point stabilization was implemented, as mentioned before. To avoid excitation laser power fluctuations, low-noise drivers were employed. Mechanical instabilities causing a changing overlap of probe and excitation laser were avoided by sturdy mounting. From Eq. 1, the theoretical influence of both last-mentioned factors can be assessed (ΔP_{eff} and Δw). Parasitic etalon effects stemming from reflections of fiber connectors were reduced by the use of index matching gel. Non-ideal behavior of the fiber-optic components (isolator, splitter, and circulator) has to be considered and they have to be chosen according to the highest possible standards. The use of an ultra-low-noise laser source in combination with a BD scheme reduces the influence of probe laser-related noise on the measurement. Finally, as only low-noise electronics were used, the relative weight of electronics noise is ranked as minute.

With the measured SNRs for each individual concentration, a mean 3σ LOD of roughly 370 ppbv (1 s integration time) could be achieved. To allow for comparison to previously reported setups, the normalized noise equivalent absorption (NNEA) is calculated, independent of the optical laser power and bandwidth. For the effective optical power P_{eff} of 40 mW and 1 s integration time, we achieve an $\text{NNEA} = \frac{\alpha P_{\text{eff}}}{\text{SNR} \sqrt{\Delta f}}$ of $1.4 \times 10^{-8} \text{ cm}^{-1} \text{ W} \sqrt{\text{Hz}}$.²⁶ Here, α is the absorption coefficient of the gas and the measurement noise bandwidth Δf was approximated by a first-order filter noise bandwidth of $\Delta f = \frac{\pi f_c}{2} = \frac{1}{4\tau_{\text{int}}}$ for the LIA's low-pass filter.²⁷ To investigate the stability of the sensor system, measurements of the background signal, with a constant flow of N₂, were performed for more than 1 hour. By calculating the Allan deviation and

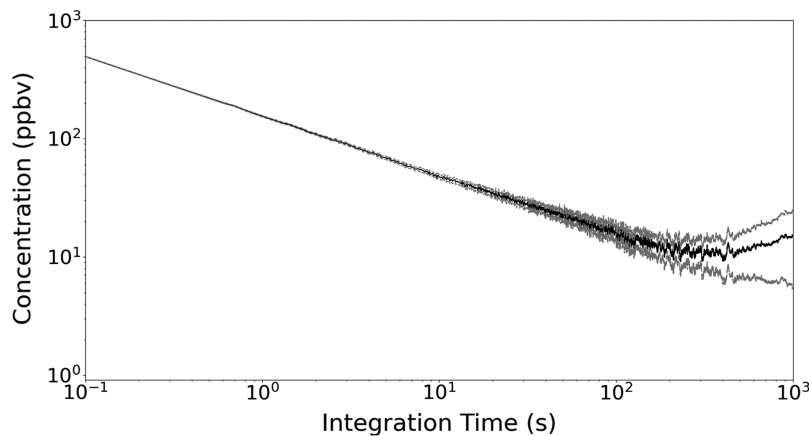


Fig. 6 The black line indicates the calculated Allan deviation in units of NO_2 concentration as measured from the background signal. The gray dotted lines depict the standard error.

converting it into units of NO_2 concentration, as shown in Fig. 6, the LOD for longer integration times can be evaluated.

The system shows good stability up to 200 s, until drift starts to dominate. With an integration time of 200 s a theoretical 3σ LOD of approximately 15 ppbv can be achieved. Similar long-term measurements of the photothermal signal with NO_2 present revealed stronger instabilities. Ongoing work indicates that additional, parasitic etalon effects, stemming from fiber-optic components and connectors, on top of the measurement FPE's transfer function, lead to varying sensitivity. Additional factors influencing the stability during a photothermal measurement are the fluctuations and drift of the excitation laser's optical power and mechanical instabilities of the setup, leading to a degradation of the overlap between probe and excitation laser.

4 Conclusions and Outlook

In this paper, an interferometric gas sensing system utilizing the photothermal effect has been presented. As a detection unit, a custom-made fiber-coupled FPE was employed, which is based on a fabrication method for low-cost fiber-coupled FPEs.¹⁶ By measuring the reflected light of the FPE, one single optical fiber is sufficient to lead light in and out of the etalon, allowing easier handling of the sensor head and simplifying the alignment process. The system was characterized with NO_2 concentrations ranging from 1 to 1000 ppmv. With 1 s integration time, a LOD of approximately 370 ppbv can be achieved. The stability of the sensor system allows for integration times up to 200 s, thereby lowering the LOD down to approximately 15 ppbv. To benchmark the system against previously published results, the NNEA was calculated to be $1.4 \times 10^{-8} \text{ cm}^{-1} \text{ W} \sqrt{\text{Hz}}$, thereby proving to be competitive, despite the used low-cost FPE. An additional advantage of the proposed sensing system is the interchangeable nature of the excitation laser source. Basically any absorbing gas or aerosol species can be detected, given the appropriate excitation laser source is available. By introducing multiple excitation beams with different wavelengths, the system could also be easily adapted for multi-gas detection. Observed instabilities of the photothermal signal are related to parasitic etalon effects, introduced by reflecting surfaces of connectors and other optical components. These effects are added on top of the FPE's transfer function, leading to signal non-linearities. Further investigations to quantify the influence of said effect are still ongoing. The use of index-matching gel reduced the effect significantly and splicing of the fiber connections is expected to suppress unwanted etalon effects below the level of detection. Effort is also put into the implementation of further excitation sources, e.g., a $4 \mu\text{m}$ interband cascade laser, to target the strong mid-infrared absorption bands of CO_2 .²⁸

Disclosures

The authors declare no conflict of interest. Relevant data can be made available by the author upon request.

Code and Data Availability

All data can be made available by the author upon request to manuel.tanzer@tugraz.at.

Acknowledgments

The work presented here was conducted in the framework of the FFG funded project “Green Sensing” and the NATO SPS program “Photonic Nano Particle Sensors for Detecting CBRN events.” The work was also supported by TU Graz Open Access Publishing Fund. Part of the content of this work has previously been presented at the SPIE Optics and Photonics conference in 2023 and can be found in the respective proceedings.²⁹

References

1. D. Popa and F. Udrea, “Towards integrated mid-infrared gas sensors,” *Sensors* **19**, 2076 (2019).
2. A. Fathy et al., “Direct absorption and photoacoustic spectroscopy for gas sensing and analysis: a critical review,” *Laser Photonics Rev.* **16**, 2100556 (2022).
3. J. Hodgkinson and R. Tatam, “Optical gas sensing: a review,” *Meas. Sci. Technol.* **24**, 012004 (2012).
4. K. Krzempek, “A review of photothermal detection techniques for gas sensing applications,” *Appl. Sci.* **9**, 2826 (2019).
5. A. J. Campillo et al., “Fabry-Perot photothermal trace detection,” *Appl. Phys. Lett.* **41**, 327–329 (1982).
6. G. Dudzik and K. Abramski, “Solid-state laser intra-cavity photothermal sensor (slips) for gas detection with parts-per-billion sensitivity,” *Eng. Proc.* **21**, 34 (2022).
7. H. Moosmüller and W. Arnott, “Folded Jamin interferometer: a stable instrument for refractive-index measurements,” *Opt. Lett.* **21**, 438–440 (1996).
8. M. Islam et al., “Chronology of Fabry-Perot interferometer fiber-optic sensors and their applications: a review,” *Sensors* **14**, 7451–7488 (2014).
9. P. Huangfu and R. Atkinson, “Long-term exposure to NO₂ and O₃ and all-cause and respiratory mortality: a systematic review and meta-analysis,” *Environ. Int.* **144**, 105998 (2020).
10. W. H. Organization, “Who global air quality guidelines,” (2021). <https://www.who.int/publications/i/item/9789240034228> (accessed 21 July 2023).
11. P. Breitegger, B. Lang, and A. Bergmann, “Intensity modulated photothermal measurements of NO₂ with a compact fiber-coupled Fabry-Pérot interferometer,” *Sensors* **19**, 3341 (2019).
12. J. P. Waclawek et al., “Balanced-detection interferometric cavity-assisted photothermal spectroscopy,” *Opt. Express* **27**, 12183–12195 (2019).
13. P. Patimisco et al., “Recent advances in quartz enhanced photoacoustic sensing,” *Appl. Phys. Rev.* **5**, 011106 (2018).
14. G. Leahu et al., “Trace gas analysis from glazes by means of a compact photothermal deflection spectroscopy apparatus,” *Rev. Sci. Instrum.* **84**, 123111 (2013).
15. M. Bertolotti and R. L. Voti, “A note on the history of photoacoustic, thermal lensing, and photothermal deflection techniques,” *J. Appl. Phys.* **128**, 230901 (2020).
16. M. Tanzer, B. Lang, and A. Bergmann, “Fabrication of a low-cost, fiber-coupled, and air-spaced Fabry-Pérot etalon,” *J. Vis. Exp.* **192**, e65174 (2023).
17. J. Chen et al., “Acoustic performance study of fiber-optic acoustic sensors based on Fabry-Pérot etalons with different Q factors,” *Micromachines* **13**, 118 (2022).
18. S. E. Bialkowski, N. G. C. Astrath, and M. A. Proskurnin, *Photothermal Spectroscopy Methods*, 2nd ed., Wiley & Sons Ltd. (2019).
19. P. Kluczynski et al., “Wavelength modulation absorption spectrometry – an extensive scrutiny of the generation of signals,” *Spectrochim. Acta Part B: At. Spectrosc.* **56**, 1277–1354 (2001).
20. I. E. Gordon et al., “The HITRAN2020 molecular spectroscopic database,” *J. Quantum Spectrosc. Radiat. Transf.* **277**, 107949 (2022).
21. M. Vaughan, *The Fabry-Perot Interferometer: History, Theory, Practice and Applications*, 1st ed., Taylor & Francis Group (1989).
22. R. Drever et al., “Laser phase and frequency stabilization using an optical resonator,” *Appl. Phys. B* **31**, 97–105 (1983).
23. P. Breitegger and A. Bergmann, “A precise gas dilutor based on binary weighted critical flows to create NO₂ concentrations,” *MDPI Proc.* **19**, 998 (2018).
24. P. Werle, R. Mücke, and F. Slemr, “The limits of signal averaging in atmospheric trace-gas monitoring by tunable diode-laser absorption spectroscopy (TDLAS),” *Appl. Phys. B* **57**, 131–139 (1993).
25. W. J. Riley, “Handbook of frequency stability analysis,” (2008). https://tsapps.nist.gov/publication/get_pdf.cfm?pub_id=50505 (accessed 19 December 2023).
26. M. Baudelet, *Laser Spectroscopy for Sensing: Fundamentals, Techniques and Applications*, Elsevier (2014).
27. C. D. Motchenbacher and J. A. Connelly, *Low-Noise Electronic System Design*, Wiley & Sons Ltd. (1993).

28. Z. Du et al., "Mid-infrared tunable laser-based broadband fingerprint absorption spectroscopy for trace gas sensing: a review," *Appl. Sci.* **9**, 338 (2019).
29. M. Tanzer, B. Lang, and A. Bergmann, "Photothermal gas sensing with a custom-made, fiber-coupled Fabry-Pérot etalon," *Proc. SPIE* **12672**, 126720D (2023).

Manuel Tanzer studied technical physics and physical energy and measurement engineering at the Vienna University of Technology (Austria). Since 2020, he is a PhD candidate at the Institute of Electrical Measurement and Sensor Systems at the Graz University of Technology (Austria). His research topic is the miniaturization of photothermal gas and aerosol sensors. He is a student-member of SPIE.

Benjamin Lang is a university assistant at the Institute for Electrical Measurement and Sensor Systems, Graz University of Technology (Austria). He received his master's degree in technical physics in 2015 and his PhD from the Faculty of Electrical and Information Engineering in 2020, both at Graz University of Technology. He is interested in and researching laser-based optical sensing techniques, focusing on laser absorption spectroscopy (tunable diode, photoacoustic, and photothermal) in gasses and condensed phases.

Matej Njegovec is an assistant professor at the University of Maribor (Slovenia) and received his BS degree in 2008. In 2013, he received his PhD in electrical engineering from the University of Maribor. His main research includes fiber optic sensors, optical sensor interrogation techniques, and the design of optoelectronic systems. He has excellent background in analog and RF circuit design, semiconductor light sources, optoelectronic components, modulation techniques, signal-processing of modulated light signals, and general signal integration techniques related to optical sensors. His biggest motive is to find innovative and cost-efficient solutions for fiber-optic sensors that would allow for the introduction of fiber-sensor technology into a broader range of practical applications.

Vedran Budinski received his BSc and PhD degrees from the Faculty of Electrical Engineering and Computer Science at the University of Maribor, Slovenia, in 2012 and 2017, respectively. Since 2012, he has been working as a researcher in the Laboratory for Electro-Optical and Sensor Systems at the University of Maribor. His research interests include fiber optic sensors for measuring twist/rotation, fiber optic microfluidic sensors, and design of miniature microstructures on the tip of an optical fiber, employing various micromachining techniques for detecting various physical and chemical parameters.

Simon Pevec is an assistant professor at the University of Maribor. In 2014, he received his PhD in electrical engineering from the University of Maribor. He has more than 15 years of researching experiences in field of photonics, optoelectronics, MOEMS, sensors, and measurements. His greatest experiences are related with fiber based Fabry-Pérot sensors, multiparameter sensors, optoelectronics system design, and micromachining of optical fibers including selective etching; all to develop all kind of miniature all-fiber Fabry-Pérot sensors and sensors systems.

Jure Javornik finished his bachelor's degree (2019) and master's degree (2022) in electrical engineering at FERI UM. During the master's degree, he was working on femtosecond laser machining procedures for fiber-optic sensor fabrication. Upon the degree completion, he started working as a junior researcher at Laboratory for Electro-Optical and Sensor Systems (LEOSS), stationed at FERI UM, where he is currently working on his PhD. His field of research includes femtosecond laser micromachining, selective etching, type 2 FBG inscription, fiber-optic sensor design, fabrication, and cost-efficient interrogation techniques.

Denis Donlagic is full professor at the University of Maribor, received his first PhD in 1998 at the University of Ljubljana (Slovenia). In 2000, he finished his second PhD at the University of Strathclyde (Glasgow, United Kingdom). He has a broad background in the fields of photonics systems, opto-electronics systems, optical fibers, and MOEMS. In particular, he has research and development experience in the fields of optical fiber sensors, optical fibers, and opto-electronics system design. His focus is in finding new scientific paradigms and technology concepts while bringing them into practical applications. He is member of IEEE and member of the editorial board of the *Journal of Lightwave Technology*.

Alexander Bergmann is professor for electronic sensor systems and head of the Institute of Electrical Measurement and Sensor Systems at Graz University of Technology. His research is dedicated to sensor effects, sensor materials, and sensor systems. One focus area is the quantification of fluid as well as aerosol properties (air pollutants and climate forcers) with emphasis on high temporal resolution. Additionally, he is laboratory head of the Christian Doppler Laboratory for Structured Matter-based Sensing, where he and his team investigate highly sensitive sensing structures based on structured light and matter.